



**HAL**  
open science

## Efficient thermomechanical analysis of functionally graded structures using the symmetric SPH method

Jiao Li, Guangchun Wang, Shuai Liu, Jun Lin, Yanjin Guan, Guoqun Zhao,  
Hakim Naceur, Daniel Coutellier, Tao Wu

► **To cite this version:**

Jiao Li, Guangchun Wang, Shuai Liu, Jun Lin, Yanjin Guan, et al.. Efficient thermomechanical analysis of functionally graded structures using the symmetric SPH method. *Case Studies in Thermal Engineering*, 2021, 25, pp.100889. 10.1016/j.csite.2021.100889 . hal-03536533

**HAL Id: hal-03536533**

**<https://uphf.hal.science/hal-03536533>**

Submitted on 25 Apr 2022

**HAL** is a multi-disciplinary open access archive for the deposit and dissemination of scientific research documents, whether they are published or not. The documents may come from teaching and research institutions in France or abroad, or from public or private research centers.

L'archive ouverte pluridisciplinaire **HAL**, est destinée au dépôt et à la diffusion de documents scientifiques de niveau recherche, publiés ou non, émanant des établissements d'enseignement et de recherche français ou étrangers, des laboratoires publics ou privés.

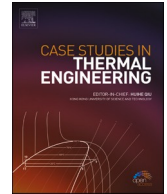


Distributed under a Creative Commons Attribution - NonCommercial - NoDerivatives 4.0 International License



Contents lists available at ScienceDirect

## Case Studies in Thermal Engineering

journal homepage: <http://www.elsevier.com/locate/csite>

## Efficient thermomechanical analysis of functionally graded structures using the symmetric SPH method

Jiao Li<sup>a,b</sup>, Guangchun Wang<sup>a</sup>, Shuai Liu<sup>a</sup>, Jun Lin<sup>a,b,\*</sup>, Yanjin Guan<sup>b,a</sup>, Guoqun Zhao<sup>a</sup>, Hakim Naceur<sup>c</sup>, Daniel Coutellier<sup>c</sup>, Tao Wu<sup>d,\*\*</sup>

<sup>a</sup> Key Laboratory for Liquid-Solid Structural Evolution & Processing of Materials (Ministry of Education), Shandong University, Jinan, 250061, China

<sup>b</sup> Suzhou Institute of Shandong University, Suzhou, 215123, China

<sup>c</sup> Laboratoire LAMIH UMR 8201, Université Polytechnique Hauts-de-France, Valenciennes, 59313, France

<sup>d</sup> Engineering Training Center, Shandong University, Jinan, 250061, China

### ARTICLE INFO

#### Keywords:

Thermoelastic analysis  
Functionally graded materials  
Meshless  
Smoothed particle hydrodynamics  
Symmetric SPH

### ABSTRACT

Tailoring the thermal and mechanical properties plays an important role in manufacturing and designing functionally graded material (FGM) which is often applied in high temperature gradient environment. The present investigation will address the basics of thermoelastic problem solved by means of a specific meshless smoothed particle hydrodynamics (SPH) method. The inconsistency of the conventional SPH method was improved by introducing the symmetric SPH (SSPH) technique, where function derivatives can be approximated by the function values in the support domain. Hence, the heat conduction and balance equations become a series of algebraic equations, which can be solved efficiently. The result accuracy achieved by the proposed approach was demonstrated in solving several numerical examples in comparison to available results in the literature. The effect of the gradation indexes on the thermoelastic behavior was also considered.

### 1. Introduction

Since the concept proposed in 1984 [1], functionally graded material (FGM) has attracted a great deal of attention and been widely used as structural elements such as turbine blades, thermal barrier coatings, rocket nozzles and so on to resist to high temperature gradients. The material properties vary gradually and continuously in space, which can be properly tailored aiming to achieve superior characteristics by adjusting the volume fraction and distribution of each constituent. Thermoelastic performance is one of the most important points to be considered in structural design, optimization and in service [2,3].

To this day, finite element method (FEM) is still one of the most powerful techniques to analyze the thermoelastic behavior of FGMs. On the basis of higher-order shear deformation theory and Green–Lagrange geometrical nonlinearity, a nonlinear FE model was developed initially to solve the large amplitude flexural behavior of functionally graded doubly curved shell panel under the thermal load [4]. Employing a double-parameter elastic foundation, Aria et al. [5] proposed a nonlocal FE model to study the thermoelastic behavior of imperfect functionally graded porous nanobeams on the basis of nonlocal elasticity theory of Eringen. Jabbari et al. [6]

\* Corresponding author. Key Laboratory for Liquid-Solid Structural Evolution & Processing of Materials (Ministry of Education), Shandong University, Jinan, 250061, China.

\*\* Corresponding author.

E-mail addresses: [linjun@sdu.edu.cn](mailto:linjun@sdu.edu.cn) (J. Lin), [wt@sdu.edu.cn](mailto:wt@sdu.edu.cn) (T. Wu).

<https://doi.org/10.1016/j.csite.2021.100889>

Received 2 September 2020; Received in revised form 13 February 2021; Accepted 14 February 2021

Available online 18 February 2021

2214-157X/© 2021 The Author(s). Published by Elsevier Ltd. This is an open access article under the CC BY-NC-ND license

(<http://creativecommons.org/licenses/by-nc-nd/4.0/>).

performed a thermoelastic analysis of the isotropic rotating FG conical shells with varying thickness using FEM in ANSYS with eight-node PLANE 223 element and a developed analytical model using a multi-layered method. Lezgy-Nazargah [7] developed a novel nonuniform rational B-splines isogeometric FE formulation based on refined higher order global-local theory to study the coupled thermomechanical response of bi-directional FGM beams. This FGM type can be effectively applied in many harsh environment with high temperature gradient since the material properties vary in two directions. Based on FEM, the thermal buckling and post-buckling analysis of functionally graded plates and cylindrical shells were performed by using the Kirchhoff–Love classical plate theory [8] and the first-order shear deformation theory (FSDT) [9,10]. The effect of the geometrical parameters, the volume fraction index, the length-to-thickness ratio and boundary conditions on nonlinear responses were investigated.

Unlike the mesh-based methods like FEM, finite volume method (FVM) [11] and finite difference method (FDM) [12], the meshless methods approximate the differential equations using the global interpolations on the discrete nodes or background mesh and thus avoid the burdensome mesh generation and re-meshing, easily monitoring the free edge and process data. Some of meshless methods have attracted the researchers’ attentions and been successfully developed for the thermoelastic analysis of FGMs [2].

Based on analog equation theory, a meshless algorithm coupling the method of fundamental solutions with radial basis functions (MFS–RBF) was proposed for the static thermal stress analysis in two-dimensional FGMs [13]. The results showed that appropriate graded parameter can reduce stress localization and the inadequate stress distribution. To facilitate the numerical solution of the boundary value problems for rather complex governing equations in FGMs, a strong form meshless formulation for solution of thin plate bending problem was developed in combination with moving least squares (MLS) approximation scheme [14]. Meshless local Petrov-Galerkin (MLPG) [15–17] method was applied for 2D functionally graded solid subjected to thermal-mechanical loads, where the penalty method is used to efficiently enforce the essential boundary conditions. Then this method was extended for the thermoelastic wave analysis in rectangular FGM domain [18] and functionally graded thick hollow cylinders [19] under transient thermal loading. The results demonstrated that the longitudinal wave speed was larger than the transverse wave speed and the wave speed was reduced from the ceramics rich side to the metal-rich side. Integrated with the FSDT [20], modified FSDT [21] and double director shell theory [22], radial point interpolation method (RPIM) was proposed to solve the static and dynamic response of functionally graded shell structures under mechanical, electrical, and thermal loads. It was found that when increasing the power law index, the deflection decreased smoothly in the electro-mechanical loading, but it grew up at first and then declined under thermal-electrical loading case. FSDT was also combined with the element-free kp-Ritz method for the deflection analysis of metal and ceramic functionally graded plates subject to thermal and mechanical loads [23]. Meshless weighted least-square (MWLS) method was extended by Zhou et al. [24] to solve the thermoelastic problems of FGM beam with interior heat source, and verified by comparing results with the solution computed from the commercial COMSOL Multiphysics software.

Among meshless methods, smoothed particle hydrodynamics (SPH) method which is a truly meshless method since it does not use any background mesh, thoroughly avoids the element distortion and re-meshing. In addition, the simple strong formulation is adopted for approximating the differential equations. These inherent advantages make SPH method efficient and easy to monitor the movement of free surface. In previous works, smoothed particle hydrodynamics (SPH) method has been extended for the bending analysis of isotropic [25], laminated composite [26] and functionally graded materials [27]. To our best knowledge, this method has not yet been applied for thermal analysis of FGMs due to the essential inconsistency problem, especially for particles at the boundaries or irregular particle distributions. Therefore, the symmetric SPH (SSPH) method [28,29] intercropping the Taylor series expansion technique was adopted in this study to improve the prediction accuracy and the thermoelastic governing equations were represented by the SPH technique. The thermoelastic behavior of transversely FG structure was analyzed and verified by comparing the referenced results in literature. The effects of the power indexes on the temperature and deformation fields are studied. Moreover, the two-directional FGM was concerned.

## 2. SPH analysis of the thermoelastic problem

In this section, the steady state thermoelastic problem of two-dimensional FGMs with isotropic linear elasticity will be carried out.

### 2.1. Heat conduction analysis of FGMs

The steady state heat conduction equation for FGMs can be stated as

$$\nabla(k(\mathbf{x})\nabla T(\mathbf{x})) + Q = 0 \tag{1}$$

where  $k$  and  $T$  are respectively the thermal conductivity and the temperature at the position  $\mathbf{x} = (x,y)$ , whereas  $Q$  is the heat resource.

Two different thermal boundary conditions are concerned.

Dirichlet boundary:

$$TT(\mathbf{x}) = \bar{T}(\mathbf{x}) , \mathbf{x} \in \Gamma_D \tag{2}$$

Neumann boundary condition

$$q_n(\mathbf{x}) = \mathbf{n} \cdot k(\mathbf{x})\nabla T(\mathbf{x}) = \bar{q}(\mathbf{x}) , \mathbf{x} \in \Gamma_N \tag{3}$$

where  $\bar{T}$  is the given temperature on the boundary  $\Gamma_D$ , and  $\bar{q}$  the prescribed heat flux on boundary  $\Gamma_N$ .  $\Gamma_D \cup \Gamma_N = \Gamma$  is the closed

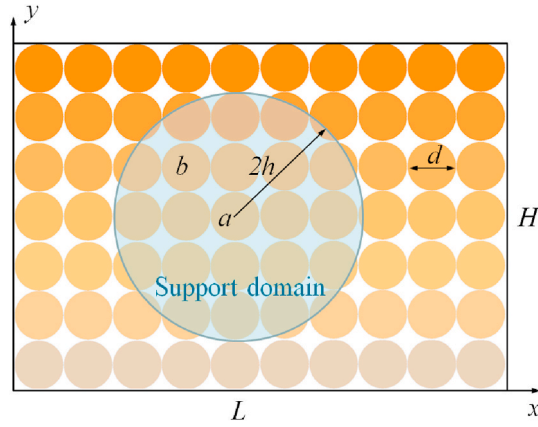


Fig. 1. 2D FGM structure with SPH particle discretization.

boundary surrounding the problem domain  $\Omega$  and  $\mathbf{n} = (n_x, n_y)$  is the outward unit normal vector.

### 2.2. Equilibrium equations of FGMs

The equilibrium equations for two-dimensional static FGMs without considering the body force can be expressed as

$$\text{div } \boldsymbol{\sigma} = 0 \tag{4}$$

where  $\boldsymbol{\sigma}$  is the Cauchy stress tensor.

Thermal stresses associated can be related to the strain  $\boldsymbol{\varepsilon}$  and temperature change  $\Delta T$  by

$$\begin{bmatrix} \sigma_{xx} \\ \sigma_{yy} \\ \sigma_{xy} \end{bmatrix} = \mathbf{C} \begin{bmatrix} \varepsilon_{xx} \\ \varepsilon_{yy} \\ 2\varepsilon_{xy} \end{bmatrix} - \beta\alpha \begin{bmatrix} 1 \\ 1 \\ 0 \end{bmatrix} \Delta T \tag{5}$$

where  $\alpha$  is the coefficient of thermal expansion,  $\beta$  is equal to  $E/(1 - \nu)$  in case of plane stress or  $E/(1 - 2\nu)$  in plane strain case. The strains  $\boldsymbol{\varepsilon}$  are determined through the displacement gradient like

$$\boldsymbol{\varepsilon} = \left[ \frac{\partial u}{\partial x} \quad \frac{\partial v}{\partial y} \quad \frac{\partial u}{\partial y} + \frac{\partial v}{\partial x} \right]^T \tag{6}$$

where  $u$  and  $v$  are the displacement in  $x$  and  $y$  direction, respectively.  $\mathbf{C}$  denotes the stiffness matrix for linearly elastic isotropic materials depending on a variable Young's modulus  $E = E(x, y)$  and a Poisson ratio  $\nu = \nu(x, y)$ . For plane stress case

$$\mathbf{C} = \frac{E}{1 - \nu^2} \begin{bmatrix} 1 & \nu & 0 \\ \nu & 1 & 0 \\ 0 & 0 & (1 - \nu)/2 \end{bmatrix} \tag{7}$$

where  $E$  and  $\nu$  are the Young's modulus and Poisson's ratio, respectively. In plane strain assumption

$$\mathbf{C} = \frac{E}{(1 + \nu)(1 - 2\nu)} \begin{bmatrix} 1 - \nu & \nu & 0 \\ \nu & 1 - \nu & 0 \\ 0 & 0 & (1 - 2\nu)/2 \end{bmatrix} \tag{8}$$

Finally substituting Eqs. (5) and (6) into Eq. (4), the balance equations can be written with respect to the displacements

$$\frac{\partial(C_{11}\varepsilon_{xx} + C_{12}\varepsilon_{yy})}{\partial x} + \frac{\partial(C_{33}\gamma_{xy})}{\partial y} = \frac{\partial(\beta\alpha\Delta T)}{\partial x} \tag{9}$$

$$\frac{\partial(C_{33}\gamma_{xy})}{\partial x} + \frac{\partial(C_{21}\varepsilon_{xx} + C_{22}\varepsilon_{yy})}{\partial y} = \frac{\partial(\beta\alpha\Delta T)}{\partial y} \tag{10}$$

From Eqs. (9) and (10), it is known that the governing function for FGMs is of much complexity, since the stiffness matrix, thermal expansion coefficient and temperature are always space dependent.

### 2.3. SPH formulation

Due to the boundary truncation of the support domain, the standard SPH encounter serious inconsistency problems. Several techniques have been proposed in the literature to improve the consistency level, like the normalized SPH (NSPH) method [30], the corrective smoothed particle method (CSPM) [31], the modified SPH (MSPH) [32] method and the symmetric SPH (SSPH) method [28, 33]. Contrary to SPH, NSPH, CSPM and MSPH, the SSPH method directly uses the smoothing functions rather than their differentials to represent the derivatives of an unknown function and thus the precision of the numerical solution of boundary-value problems is improved. In the following, the SSPH method is briefly introduced.

Considering a two-dimensional FGM structure, the domain is discretized by  $N$  SPH particles as presented in Fig. 1. Each particle contains the information such as the position, density, temperature, displacement, thermal conductivity, Young's modulus, stress, strain and so on.

Assuming a position related function  $f(\mathbf{x})$  owning  $(m+1)$ -times differentiability, the function value at point  $b$  with coordinates  $\mathbf{x}_b = (x_b, y_b)$  can be estimated through Taylor series expansion,

$$f(\mathbf{x}_b) = P_m(\mathbf{x}_b) = \sum_{r=0}^m \sum_{s=0}^r \frac{C_r^s}{r!} (x_b - x_a)^s (y_b - y_a)^{r-s} \left. \frac{\partial^r f}{\partial x^s \partial y^{r-s}} \right|_{\mathbf{x}_a} \quad (11)$$

where  $a$  is the neighboring point of  $b$ ,  $m$  is the Taylor polynomial degree,  $r$  and  $s$  are integers depending on the degree order of Taylor polynomial given by  $r = 0, 1, 2, \dots, m$  and  $s = 0, 1, 2, \dots, r$

Since only the terms from 0-th to 2nd order are needed in the heat transfer equation (1) and balance equations 9 and 10, therefore the higher order terms in Eq. (11) will not be considered in the following. Eq (11) can be re-expressed using the matrix form as

$$f(\mathbf{x}_b) = \mathbf{p}(\mathbf{x}_b, \mathbf{x}_a) \cdot \mathbf{q}(\mathbf{x}_a)^T \quad (12)$$

where,  $\mathbf{p}(\mathbf{x}_b, \mathbf{x}_a)$  is the polynomial basis of approximation

$$\mathbf{p}(\mathbf{x}_b, \mathbf{x}_a) = \{1, x_b - x_a, y_b - y_a, (x_b - x_a)^2, (y_b - y_a)^2, (x_b - x_a)(y_b - y_a)\} \quad (13)$$

$$\mathbf{q}(\mathbf{x}_a) = \{f, f_x, f_y, f_{xx}/2, f_{yy}/2, f_{xy}\} \Big|_{\mathbf{x}_a} \quad (14)$$

Both sides of Eq. (12) are multiplied with  $W(\mathbf{x}_b, \mathbf{x}_a)\mathbf{p}(\mathbf{x}_b, \mathbf{x}_a)^T$ , achieving a symmetric matrix times for the vector  $\mathbf{q}(\mathbf{x})$  leading to

$$f(\mathbf{x}_b)W(\mathbf{x}_b, \mathbf{x}_a)\mathbf{p}(\mathbf{x}_b, \mathbf{x}_a)^T = \mathbf{p}(\mathbf{x}_b, \mathbf{x}_a)^T W(\mathbf{x}_b, \mathbf{x}_a)\mathbf{p}(\mathbf{x}_b, \mathbf{x}_a)\mathbf{q}^T(\mathbf{x}_a) \quad (15)$$

where  $W(\mathbf{x}_b, \mathbf{x}_a)$  is a smoothing function usually used in SPH method, determining the support domain of the interested particle. Situated in the support domain of the particle  $\mathbf{x}_a$ , there are  $N_a$  neighboring particles  $\mathbf{x}_b$  with effective contribution. Therefore, when changing neighboring particles  $\mathbf{x}_b$  in Eq. (15), we obtain  $N_a$  equations. Summing these equations, it results,

$$\sum_{b=1}^{N_a} f(\mathbf{x}_b)W(\mathbf{x}_b, \mathbf{x}_a)\mathbf{p}(\mathbf{x}_b, \mathbf{x}_a)^T = \sum_{b=1}^{N_a} \mathbf{p}(\mathbf{x}_b, \mathbf{x}_a)^T W(\mathbf{x}_b, \mathbf{x}_a)\mathbf{p}(\mathbf{x}_b, \mathbf{x}_a)\mathbf{q}^T(\mathbf{x}_a) \quad (16)$$

Finally  $\mathbf{q}^T(\mathbf{x}_a)$  including function and its derivatives at position  $\mathbf{x}_a$  can be solved by inverting a symmetric matrix,

$$\mathbf{q}^T(\mathbf{x}_a) = \left[ \sum_{b=1}^{N_a} \mathbf{p}(\mathbf{x}_b, \mathbf{x}_a)^T W(\mathbf{x}_b, \mathbf{x}_a)\mathbf{p}(\mathbf{x}_b, \mathbf{x}_a) \right]^{-1} \sum_{b=1}^{N_a} \mathbf{p}(\mathbf{x}_b, \mathbf{x}_a)^T W(\mathbf{x}_b, \mathbf{x}_a)f(\mathbf{x}_b) = \sum_{b=1}^{N_a} s(\mathbf{x}_a, \mathbf{x}_b)f(\mathbf{x}_b) \quad (17)$$

where  $s_{ab} = s(\mathbf{x}_a, \mathbf{x}_b) = \left[ \sum_{b=1}^{N_a} \mathbf{p}(\mathbf{x}_b, \mathbf{x}_a)^T W(\mathbf{x}_b, \mathbf{x}_a)\mathbf{p}(\mathbf{x}_b, \mathbf{x}_a) \right]^{-1} \mathbf{p}(\mathbf{x}_b, \mathbf{x}_a)^T W(\mathbf{x}_b, \mathbf{x}_a)$ .

From Eq. (17), it can be noticed that all spatial derivatives of the function  $f$  can be approximated by the function values of the neighboring particles, such as

$$\left\{ \begin{aligned} f_a &= q_{1a} = \sum_{b=1}^{N_a} s_{1ab} f_b \\ f_{a,x} &= q_{2a} = \sum_{b=1}^{N_a} s_{2ab} f_b \\ f_{a,y} &= q_{3a} = \sum_{b=1}^{N_a} s_{3ab} f_b \\ f_{a,xx} &= q_{4a} = 2 \sum_{b=1}^{N_a} s_{4ab} f_b \\ f_{a,yy} &= q_{5a} = 2 \sum_{b=1}^{N_a} s_{5ab} f_b \\ f_{a,xy} &= q_{6a} = \sum_{b=1}^{N_a} s_{6ab} f_b \end{aligned} \right. \quad (18)$$

The kernel function  $W$  adopted in the present work is the well known cubic B-spline function [25].

$$W(x_b, x_a) = \frac{15}{7\pi h^2} \begin{cases} 1 - \frac{3}{2}l^2 + \frac{3}{4}l^3 & 0 \leq l < 1 \\ \frac{1}{6}(2-l)^3 & 1 \leq l < 2 \\ 0 & 2 \leq l \end{cases} \quad (19)$$

where  $l = |x_b - x_a|/h$  and  $h$  is the smoothing length. The radius of the support domain is  $2h$ .

#### 2.4. SPH implementation for thermoelastic problem in FGMs

In FGMs, the parameters such as thermal conductivity, thermal expansion coefficient, Young’s modulus and Poisson’s ratio are varied with the particle location, and their derivatives can be evaluated by their explicit definition related to the particle coordinates. However the unknown variables such as temperature and displacements as well as their derivatives are necessitated to be computed using the proposed SPH method by the corresponding variable value at the neighboring particles. Therefore through Eq. (18), the heat conduction equation (1) at the particle  $a$  can be transformed to a series of linear algebraic equations, like

$$\left[ k_{a,x} \sum_{b=1}^{N_a} s_{2ab} + k_{a,y} \sum_{b=1}^{N_a} s_{3ab} + 2k_a \left( \sum_{b=1}^{N_a} s_{4ab} + \sum_{b=1}^{N_a} s_{5ab} \right) \right] T_b = -Q_a \quad (20)$$

Once the temperature change is calculated by solving Eq. (20), the balance equations 9 and 10 related to the temperature can be rewritten using the proposed SPH method, as

$$\left[ C_{11a,x} \sum_{b=1}^{N_a} s_{2ab} + 2C_{11a} \sum_{b=1}^{N_a} s_{4ab} + C_{33a,y} \sum_{b=1}^{N_a} s_{3ab} + 2C_{33a} \sum_{b=1}^{N_a} s_{5ab} \right] u_b + \left[ C_{12a,x} \sum_{b=1}^{N_a} s_{3ab} + C_{12a} \sum_{b=1}^{N_a} s_{6ab} + C_{33a,y} \sum_{b=1}^{N_a} s_{2ab} + C_{33a} \sum_{b=1}^{N_a} s_{6ab} \right] v_b = \beta_{a,x} \alpha_a \Delta T_a + \beta_a \alpha_{a,x} \Delta T_a + \beta_a \alpha_a \sum_{b=1}^{N_a} s_{2ab} \Delta T_b \quad (21)$$

$$\left[ C_{21a,y} \sum_{b=1}^{N_a} s_{2ab} + C_{21a} \sum_{b=1}^{N_a} s_{6ab} + C_{33a,x} \sum_{b=1}^{N_a} s_{3ab} + C_{33a} \sum_{b=1}^{N_a} s_{6ab} \right] u_b + \left[ C_{22a,y} \sum_{b=1}^{N_a} s_{3ab} + 2C_{22a} \sum_{b=1}^{N_a} s_{5ab} + C_{33a,x} \sum_{b=1}^{N_a} s_{2ab} + C_{33a} 2 \sum_{b=1}^{N_a} s_{4ab} \right] v_b = \beta_{a,y} \alpha_a \Delta T_a + \beta_a \alpha_{a,y} \Delta T_a + \beta_a \alpha_a \sum_{b=1}^{N_a} s_{3ab} \Delta T_b \quad (22)$$

So far, the equilibrium function is also changed to a series of linear algebraic equations, which can be easily solved by numerical method.

### 3. Numerical applications

Two numerical examples using different micromechanical characteristics and boundary conditions will be solved to show the efficiency of the proposed procedure. In the first application, a clamped-clamped FGM beam is considered to verify the proposed SPH method by comparing to the solution available in literature. Then the thermoelastic analysis of a bi-directional FGM plate with different gradation exponents is performed.

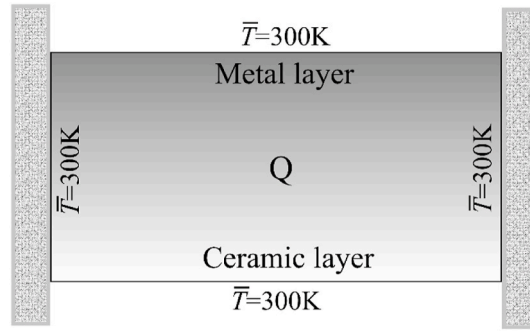


Fig. 2. Clamped-clamped FG beam with internal heat resource.

**Table 1**  
Material properties of material composition of the FG beam.

Material properties	Al	SiC
Thermal conductivity, $k$ (W/m•K)	233	65
Young's modulus, $E$ (GPa)	70	427
Poisson's ratio, $\nu$	0.3	0.17
Thermal expansion coefficient, $\alpha$ (/K)	2.34E-5	4.3E-6

**Table 2**  
Temperature and x-displacement obtained by SPH and COMSOL.

Method	Maximum	x-displacement (mm)	
	Temperature (K)	Maximum	Minimum
SPH ( 6 × 3 )	362.3	1.889	-1.889
SPH ( 11 × 6 )	359.2	0.903	-0.903
SPH ( 21 × 11 )	361.2	0.747	-0.747
SPH ( 31 × 16 )	360.1	0.660	-0.660
SPH ( 41 × 21 )	361.1	0.623	-0.623
COMSOL [24]	361.1	0.639	-0.639

### 3.1. Clamped-clamped FG beam

Fig. 2 shows a FG beam with a length  $L = 1$  m and a width  $H = 0.5$  m. The left and right edges are clamped. A predefined temperature of 300 K is assigned at the four edges with an interior heat resource  $Q$ .

The beam is composed of a metallic upper region made of Al and a lower region made of ceramic SiC, where material properties are summarized in Table 1. The volume fraction of the metallic region follows a power law and is determined by a power index  $\gamma$  in the width direction as  $V_m = (y/H)^\gamma$ , thus the volume fraction of the ceramic is  $V_c = 1 - V_m$ .

The effective material properties are homogenized and determined by the Mori-Tanaka model, they are as follows

$$\left\{ \begin{aligned} k &= k_m + \frac{3k_m V_c (k_c - k_m)}{3k_m + V_m (k_c - k_m)} \\ k &= K_m + \frac{V_c (3K_m + 4G_m)(K_c - K_m)}{3(1 - V_c)(K_c - K_m) + 3K_m + 4G_m} \\ G &= G_m + \frac{V_c (G_m + \lambda)(G_c - G_m)}{(1 - V_c)(G_c - G_m) + G_m + \lambda} \\ E &= \frac{9KG}{3K + G}, \nu = \frac{3K - 2G}{2(3K + G)} \\ \alpha &= \alpha_m + \frac{E_c (E_m - E)(\alpha_c - \alpha_m)}{E(E_m - E_c)} \end{aligned} \right. \quad (23)$$

where  $K, G$  are the bulk and shear moduli.  $\lambda = G_m(9E_m + 8G_m)/6(E_m + 2G_m)$ .

First, the developed SPH method was verified by comparing to the reference solution [24] of the FE method using the software COMSOL Multiphysics and the meshless weighted least-square method (MWLS) method. The gradation index  $\gamma$  was set as zero and thus the material is considered as a pure metal. The beam was discretized by  $6 \times 3, 11 \times 6, 21 \times 11, 31 \times 16$  and  $41 \times 21$  particles,

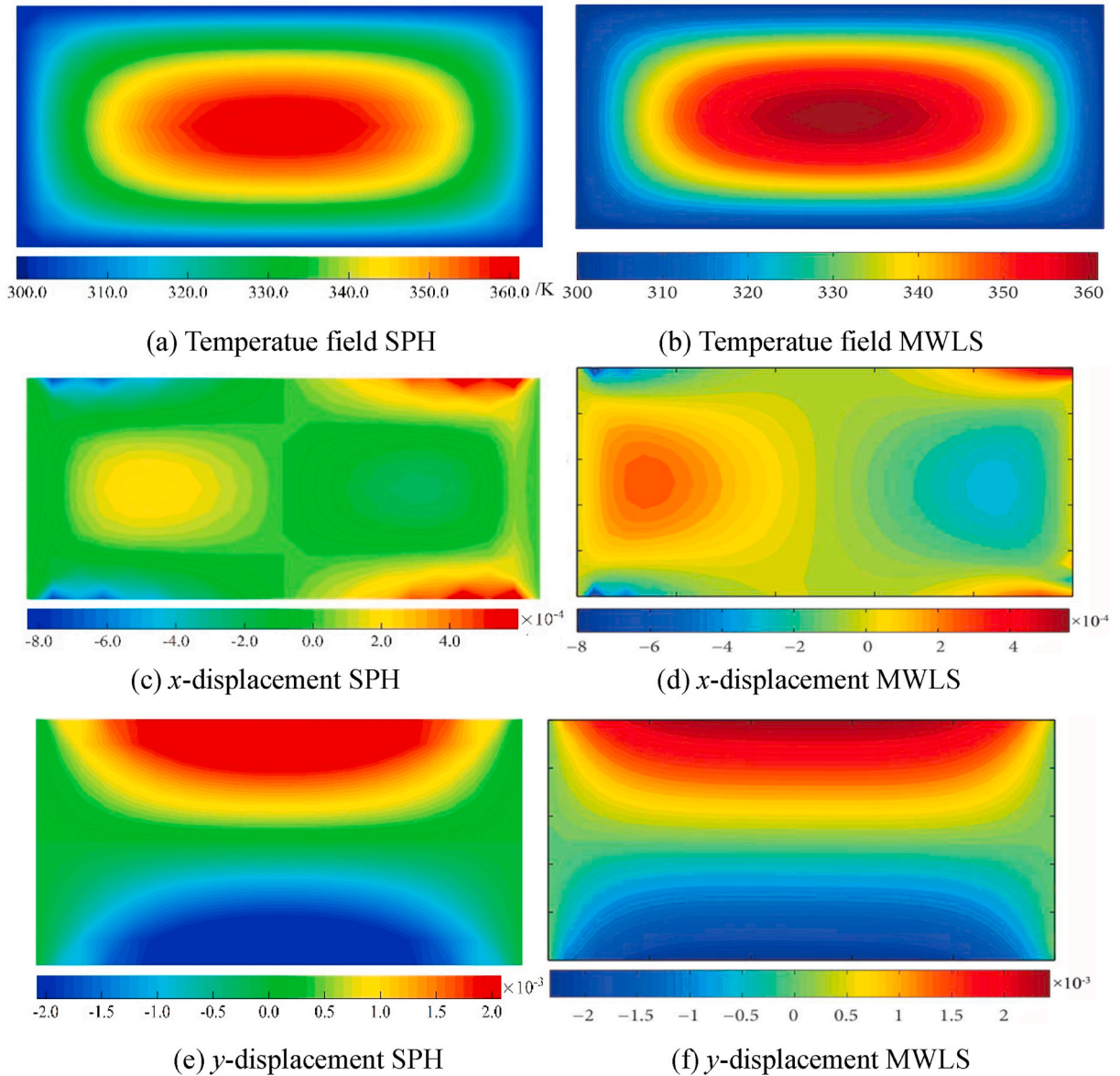


Fig. 3. Comparison between the SPH and the MWLS at  $\gamma = 0$ .

corresponding to the particle distance of 200 mm, 100 mm, 50 mm, 33.3 mm and 25 mm, respectively. The heat source considered in this study was fixed to  $Q = 5E5 \text{ W/m}^3$ . The maximum temperature and the extreme longitudinal displacement predicted by the proposed method are summarized in Table 2, together with the COMSOL solution obtained by 948 triangle mesh [24].

From Table 2, it can be noticed that by refining the particles discretization, the temperature and displacements converge to the reference solution of FE method. It can be remarked that even with a very coarse particles discretization of the proposed method, the temperature was accurately predicted with a relative error less than 0.33%. The finest particles discretization  $41 \times 21$  used in this study gave the same temperature as the reference value and the predicted displacement error was less than 2.5%. The accuracy of the obtained results based on a coarse discretization proves the effectiveness of the proposed SPH model.

The profile contours of the temperature and displacement obtained by the present SPH method and the reference solution of MWLS method are displayed in Fig. 3.

From Fig. 3, it can be noticed that the distribution regularity of the predicted temperature and displacement are similar to the results obtained by the MWLS [24]. The maximum temperature is localized at the beam centroid. The SPH method verifies the symmetry condition, the longitudinal displacement is right-and-left symmetrical but the transverse displacement is up-down asymmetrical. The predicted displacement at the centroid is zero and hence the symmetry condition due to boundary conditions is respected.

**Table 3**  
Maximum temperatures at different indices and heat sources.

Gradation index	SSPH ( 21 × 11 )		MWLS ( 31 × 15 ) [24]	
	$Q = 5 \times 10^5 \text{W/m}^3$	$Q = 5 \times 10^6 \text{W/m}^3$	$Q = 5 \times 10^5 \text{W/m}^3$	$Q = 5 \times 10^6 \text{W/m}^3$
$\gamma = 0$	361.2	912.2	361.8	910.8
$\gamma = 2$	435.2	1651.9	425.6	1558.2
$\gamma = 3$	449.6	1795.8	436.1	1660.9

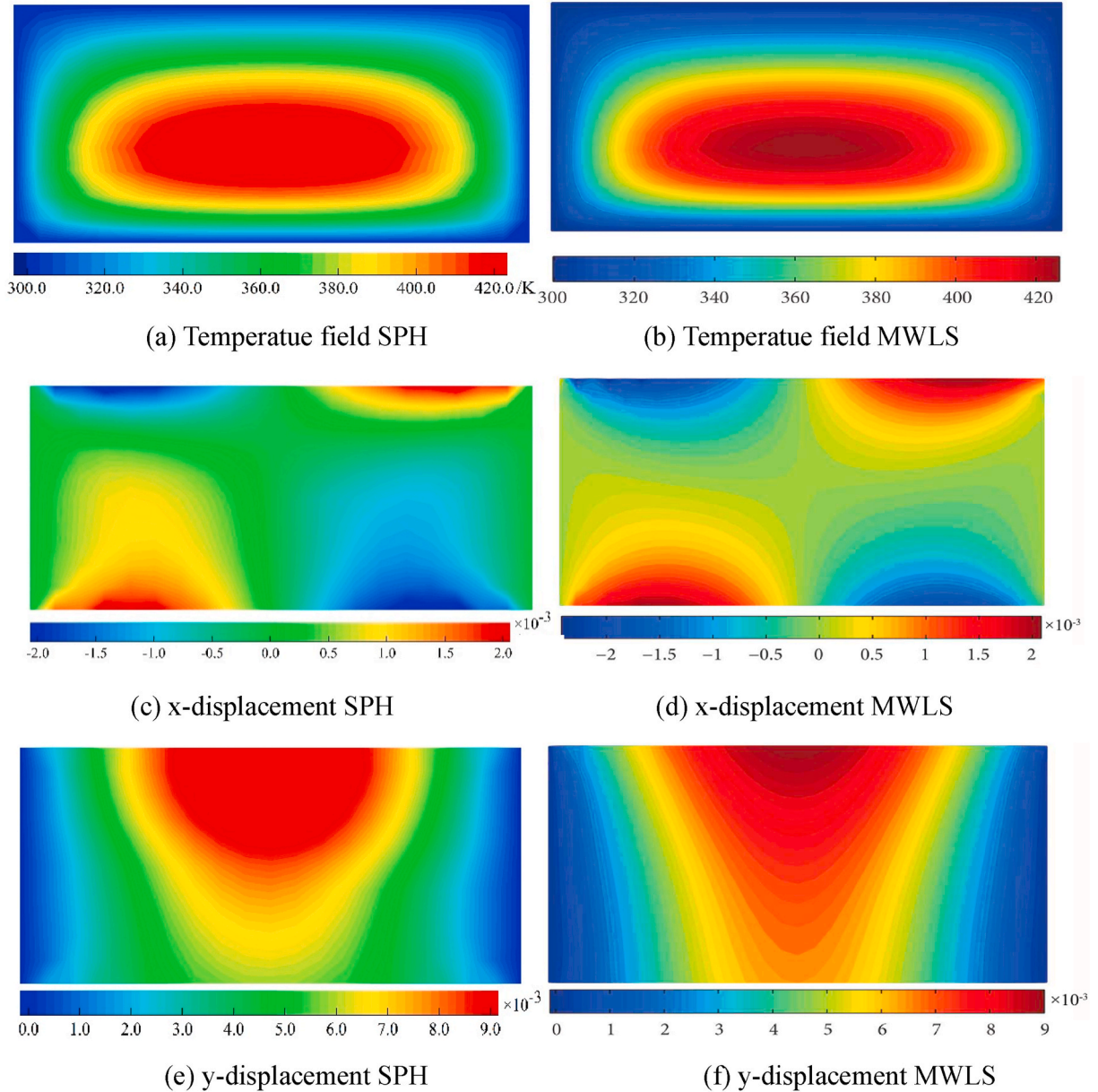


**Fig. 4.** Comparing the results obtained by SPH and MWLS at  $\gamma = 2$ .

The analysis of this example allows the study of the dependence of the gradation index upon the material properties, the internal heat source on the temperature and displacement fields. Table 3 summarizes the extreme temperatures obtained by SPH and MWLS methods.

From Table 3, we can remark the good agreement between the temperatures of SPH and MWLS, for all combination of the gradation

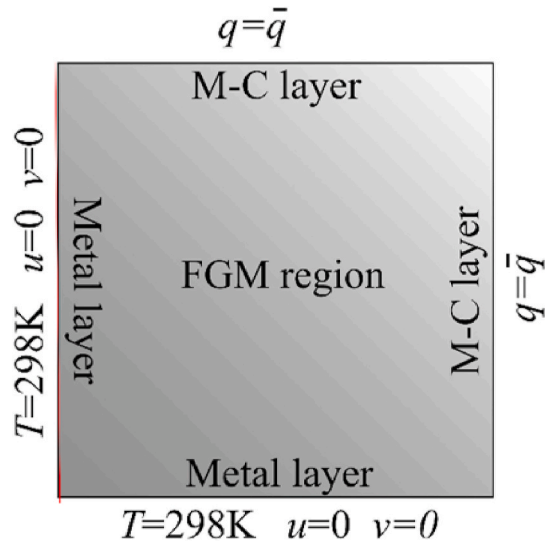


Fig. 5. Bi-directional FG square plate with heat flux.

**Table 4**  
Material properties of the FG plate.

Material properties	Ni	Al <sub>2</sub> O <sub>3</sub>
Thermal conductivity, $k$ (W/m•K)	60.5	46
Shear modulus, $G$ (GPa)	76	150
Bulk modulus, $K$ (GPa)	180	172
Thermal expansion coefficient, $\alpha$ (/K)	6.6E-6	8.1E-6

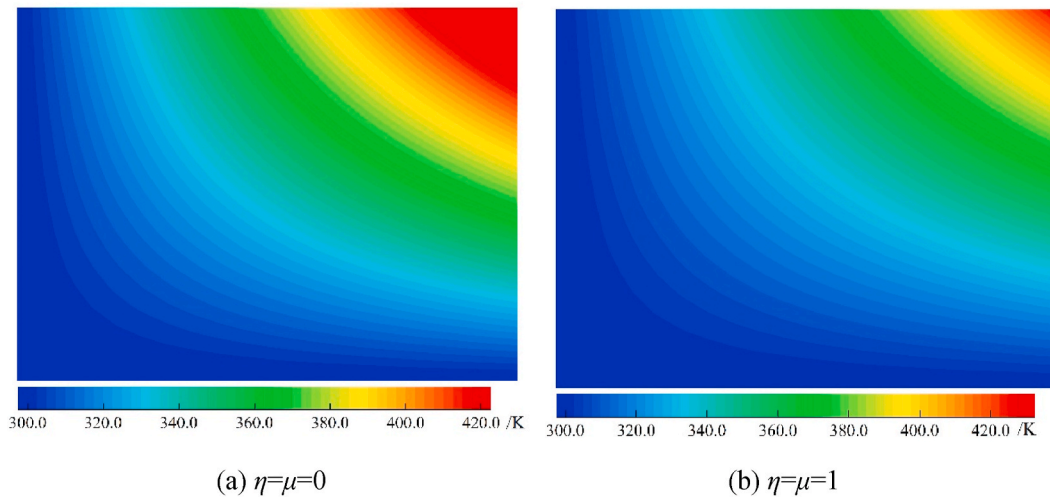


Fig. 6. Temperature distribution in the FG plate.

index and internal heat source. By increasing the gradation index and the heat source, the maximal temperature grows since more ceramic is inside the beam with more heat energy.

Fig. 4 shows temperature and displacement contours for  $\gamma = 2$  obtained by the proposed SPH and MWLS method.

From Fig. 4, it can be noticed the good correlation of the temperature, and displacement fields between SPH and MWLS. The localized maximal temperature travels to the bottom side of the beam where ceramic with higher heat conductivity is dominating.

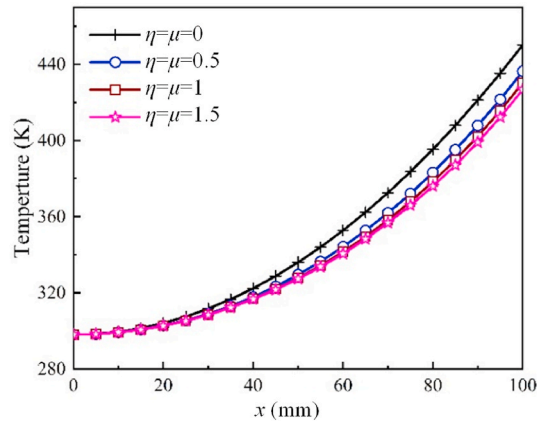


Fig. 7. Temperature distribution along the diagonal.

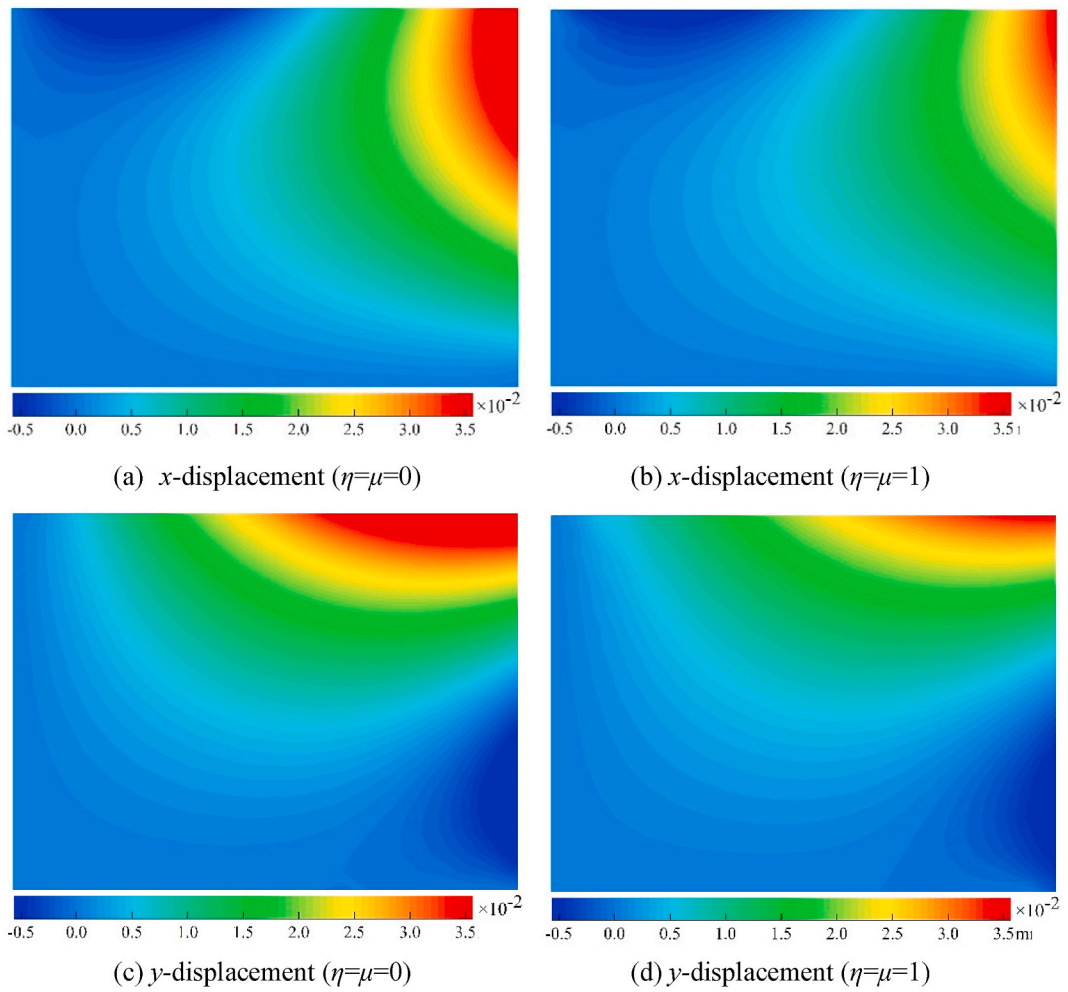


Fig. 8. Displacement distribution in the FG plate.

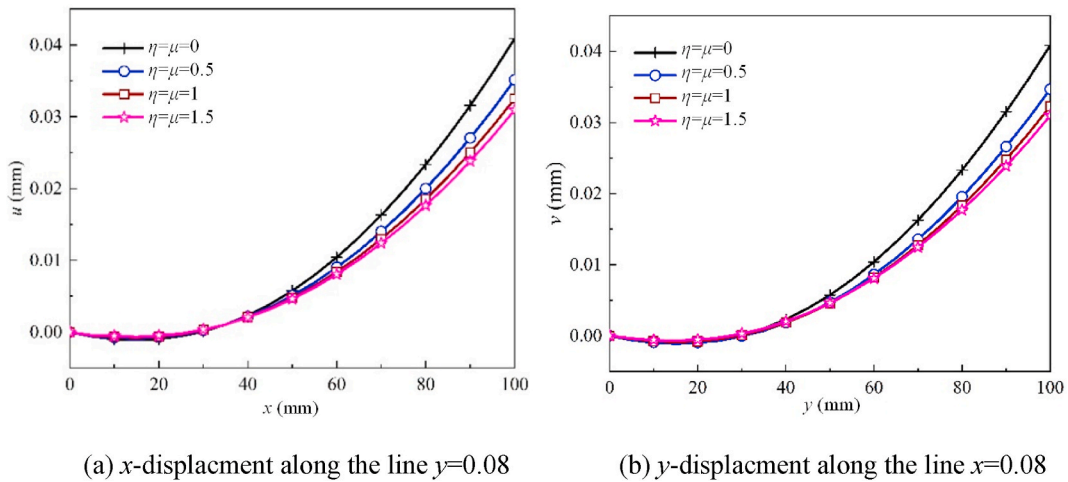


Fig. 9. Displacement distribution for  $x = 0.08$  m and for  $y = 0.08$  m

### 3.2. Bi-directional FG square plate

Fig. 5 shows the thermomechanical problem of a bi-directional FG square plate with an edge length  $L = H = 0.1$  m. The left and bottom edges are clamped and the Dirichlet condition on the temperature is fixed as  $T = 298$  K. On the right and upper edges, the free displacement boundary condition and the heat flux  $\bar{q} = 70$  kW/m<sup>2</sup> normal to the edge are applied.

The plate is constituted by Ni and Al<sub>2</sub>O<sub>3</sub> materials where mechanical and thermal properties [34] are summarized in Table 4.

The volume fraction of the ceramic varies simultaneously in the axial and thickness directions like  $V_c(x, y) = (x/L)^\eta (y/H)^\mu$ , wherein  $\eta$  and  $\mu$  define the power gradation indexes along  $x$  and  $y$  directions, respectively. In this case, the metal volume ratio is  $V_m(x, y) = 1 - V_c(x, y)$  and the material properties  $P$  of the FGM can be computed by the power law  $P = V_c P_c + V_m P_m$ .

In the SPH prediction, the plate is discretized using  $21 \times 21$  uniformly distributed particles with the overall particle distance of 5 mm. The gradation indexes are assumed to be identical and the value is set to be 0, 0.5, 1 and 1.5. Firstly, the heat conduction analysis is performed. Fig. 5 depicts the temperature profile contours when  $\eta = \mu = 0$  and  $\eta = \mu = 1$ . To clearly understand the effects of the gradation index on the temperature distribution, the temperatures along the diagonal line are given in Fig. 6.

From Fig. 6, it can be remarked that the highest temperature zone is smaller in the bi-directional FG plate (Fig. 6b) when compared to the pure ceramic plate (Fig. 6a). From Fig. 7 drawing the temperatures along the line  $y = x$ , we can observe that the temperature firstly gradually increases and then quickly rises along the diagonal from the left bottom corner to the right top vertex, where the heat enters. While increasing the gradation indexes, the maximum temperature on the upper right corner decreases since more metal rich in the plate.

Then the thermoelastic deformation of the FG plate is investigated. The displacements in axial and thickness directions are shown in Fig. 8 when  $\eta = \mu = 0$  and  $\eta = \mu = 1$ .

From Fig. 8, it can be noticed that maximum displacements are localized in the top right corner where the temperature is the highest. When the volume fraction parameters are 1, the displacements become smaller and the large deformation area decreases comparing to the case of  $\eta = \mu = 0$ .

Fig. 9 shows the effect of the gradation exponents on the displacements for  $x = 0.08$  m and for  $y = 0.08$  m, the displacements reduce with the increase of the gradation exponents. The growth becomes slow and the displacement would be saturated with continuously increasing the exponents.

## 4. Conclusions

In this investigation, a meshless model for the thermomechanical analysis of FG beam is developed based on SPH method. The results of the standard SPH method was improved by SSPH technique, which is easy and straightforward in its formulation and numerical development. The thermomechanical solution of some FG applications were analyzed using the developed SPH method and verified by comparison to reference solutions from the literature. Different material models, boundary conditions and gradation indexes have been studied. The proposed method has shown to be a good alternative tool for the thermomechanical analysis for FGMs, which could be a useful for their design and optimization.

### CRedit authorship contribution statement

Jiao Li: Methodology, Validation, Visualization, Writing – original draft. Guangchun Wang: Funding acquisition, Investigation. Shuai Liu: Formal analysis. Jun Lin: Conceptualization, Supervision, Writing – review & editing. Yanjin Guan: Project

administration, Resources. **Guoqun Zhao**: Data curation. **Hakim Naceur**: Conceptualization, Writing – review & editing. **Daniel Coutellier**: Validation, Writing – review & editing. **Tao Wu**: Validation.

### Declaration of competing interest

The authors declare that they have no known competing financial interests or personal relationships that could have appeared to influence the work reported in this paper.

### Acknowledgements

This project is supported by National Natural Science Foundation of China (Grant No. 52005299, 51705291), and Young Scholars Program of Shandong University.

### References

- [1] M. Koizumi, The concept of FGM, *Trans. Am. Ceram. Soc.* 34 (1993) 3–10.
- [2] K. Swaminathan, D.M. Sangeetha, Thermal analysis of FGM plates – a critical review of various modeling techniques and solution methods, *Compos. Struct.* 160 (2017) 43–60.
- [3] M. Damadam, R. Moheimani, H. Dalir, Bree's diagram of a functionally graded thick-walled cylinder under thermo-mechanical loading considering nonlinear kinematic hardening, *Case Stud. Therm. Eng.* 12 (2018) 644–654.
- [4] V.J. Kar, S.K. Panda, Thermoelastic analysis of functionally graded doubly curved shell panels using nonlinear finite element method, *Compos. Struct.* 129 (2015) 202–212.
- [5] A.I. Aria, T. Rabczuk, M.I. Friswell, A finite element model for the thermoelastic analysis of functionally graded porous nanobeams, *Eur. J. Mech. Solid.* 77 (2019), 103767.
- [6] M. Jabbari, M.Z. Nejad, M. Ghannad, Thermoelastic analysis of axially functionally graded rotating thick truncated conical shells with varying thickness, *Compos. Part B* 96 (2016) 20–34.
- [7] M. Lezgy-Nazargah, Fully coupled thermo-mechanical analysis of bi-directional FGM beams using NURBS isogeometric finite element approach, *Aero. Sci. Technol.* 45 (2015) 154–164.
- [8] S. Trabelsi, S. Zgha, F. Dammak, Thermo-elastic buckling and post-buckling analysis of functionally graded thin plate and shell structures, *J. Braz. Soc. Mech. Sci.* 42 (2020) 233.
- [9] S. Trabelsi, A. Frikha, S. Zgha, F. Dammak, A modified FSDT-based four nodes finite shell element for thermal buckling analysis of functionally graded plates and cylindrical shells, *Eng. Struct.* 178 (2019) 444–459.
- [10] S. Trabelsi, A. Frikha, S. Zgha, F. Dammak, Thermal post-buckling analysis of functionally graded material structures using a modified FSDT, *Int. J. Mech. Sci.* 144 (2018) 74–89.
- [11] J.F. Gong, L.K. Xuan, P.J. Ming, W.P. Zhang, Thermoelastic analysis of functionally graded solids using a staggered finite volume method, *Compos. Struct.* 104 (2013) 134–143.
- [12] M.D. Demirbaş, R. Ekici, M.F. Apalak, Thermoelastic analysis of temperature-dependent functionally graded rectangular plates using finite element and finite difference methods, *Mech. Adv. Mater. Struct.* 27 (9) (2020) 707–724.
- [13] H. Wang, Q.H. Qin, Meshless approach for thermo-mechanical analysis of functionally graded materials, *Eng. Anal. Bound. Elem.* 32 (2008) 704–712.
- [14] L. Sator, V. Sladek, J. Sladek, Bending of FGM plates under thermal load: classical thermoelasticity analysis by a meshless method, *Compos. Part B* 146 (2018) 176–188.
- [15] H.K. Ching, S.C. Yen, Meshless local Petrov-Galerkin analysis for 2D functionally graded elastic solids under mechanical and thermal loads, *Compos. Part B* 36 (2005) 223–240.
- [16] S.M. Hosseini, J. Sladek, V. Sladek, Two dimensional transient analysis of coupled non-Fick diffusion- thermoelasticity based on Green-Naghdi theory using the meshless local Petrov-Galerkin (MLPG) method, *Int. J. Mech. Sci.* 82 (2014) 74–80.
- [17] S.M. Hosseini, M.H. Ghadiri Rad, Application of meshless local integral equations for two-dimensional transient coupled hygrothermoelasticity analysis: moisture and thermoelastic wave propagations under shock loading, *J. Therm. Stresses* 40 (1) (2017) 40–54.
- [18] R.A. Akbari, A. Bagri, S.P.A. Bordas, T. Rabczuk, Analysis of thermoelastic waves in a two-dimensional functionally graded materials domain by the meshless local petrov-galerkin (MLPG) method, *CMES-Comp. Model. Eng.* 65 (1) (2010) 27–74.
- [19] S.M. Hosseini, F. Shahabian, J. Sladek, V. Sladek, Stochastic meshless local petrov-galerkin (MLPG) method for thermo-elastic wave propagation analysis in functionally graded thick hollow cylinders, *CMES-Comp. Model. Eng.* 71 (1) (2011) 39–66.
- [20] H. Nourmohammadi, B. Behjat, Static analysis of functionally graded piezoelectric plates under electro-thermo-mechanical loading using a meshfree method based on RPIM, *J. Stress Anal.* 4 (2) (2019) 93–106.
- [21] H. Mellouli, H. Jrad, M. Wali, F. Dammak, Free vibration analysis of FG-CNTRC shell structures using the meshfree radial point interpolation method, *Comput. Math. Appl.* 79 (2020) 3160–3178.
- [22] H. Mellouli, H. Jrad, M. Wali, F. Dammak, Geometrically nonlinear meshfree analysis of 3D-shell structures based on the double directors shell theory with finite rotations, *Steel Compos. Struct.* 31 (4) (2019) 397–408.
- [23] Y.Y. Lee, X. Zhao, K.M. Liew, Thermoelastic analysis of functionally graded plates using the element-free, kp-Ritz method 18 (3) (2009), 035007.
- [24] H.M. Zhou, X.M. Zhang, Z.Y. Wang, Thermal analysis of 2D FGM beam subjected to thermal loading using meshless weighted least-square method, *Math. Probl. Eng.* (2019) 2541707.
- [25] J. Lin, H. Naceur, D. Coutellier, A. Laksimi, Efficient meshless SPH method for the numerical modeling of shell structures undergoing large deformations, *Inter. J. Nonlin. Mech.* 65 (2014) 1–13.
- [26] J. Lin, H. Naceur, A. Laksimi, D. Coutellier, On the implementation of a nonlinear shell-based SPH method for thin multilayered structures, *Compos. Struct.* 108 (2014) 905–914.
- [27] J. Li, Y. Guan, G. Wang, G. Zhao, J. Lin, H. Naceur, D. Coutellier, Meshless modeling of bending behavior of bi-directional functionally graded beam structures, *Compos. Part B* 155 (2018) 104–111.
- [28] R.C. Batra, G.M. Zhang, SSPH basis functions for meshless methods, and comparison of solutions with strong and weak formulations, *Comput. Mech.* 41 (2008) 527–545.
- [29] A. Karamanli, Elastostatic analysis of two-directional functionally graded beams using various beam theories and symmetric smoothed particle hydrodynamics method, *Compos. Struct.* 160 (2017) 653–669.
- [30] P.W. Randles, L.D. Libersky, Smoothed particle hydrodynamics: some recent improvements and applications, *Comput. Methods Appl. Mech. Eng.* 139 (1) (1996) 375–408.
- [31] J.K. Chen, J.E. Beraun, T.C. Carney, A corrective smoothed particle method for boundary value problems in heat conduction, *Int. J. Numer. Methods Eng.* 46 (1999) 231–252.

- [32] R.C. Batra, G.M. Zhang, Modified Smoothed Particle Hydrodynamics (MSPH) basis functions for meshless methods, and their application to axisymmetric Taylor impact test, *J. Comput. Phys.* 227 (2008) 1962–1981.
- [33] S. Liu, J. Li, L. Chen, Y. Guan, C. Zhang, F. Gao, J. Lin, Solving 2D Poisson-type equations using meshless SPH method, *Results Phys* 13 (2019), 102260.
- [34] M.K. Apalak, M.D. Demirbas, Thermal stress analysis of in-plane two-directional functionally graded plates subjected to in-plane edge heat fluxes, *P. I. Mech. Eng. L-J. Mat.* 232 (8) (2018) 693–716.